*Science in China Series E: Technological Sciences*



www.scichina.com
tech.scichina.com
www.springerlink.com

# Fabrication of metal suspending nanostructures by nanoimprint lithography (NIL) and isotropic reactive ion etching (RIE)

XIE GuoYong[1,2†], ZHANG Jin[1], ZHANG YongYi[1], ZHANG YingYing[1], ZHU Tao[1] & LIU ZhongFan[1†]

[1] Center for Nanoscale Science and Technology (CNST), College of Chemistry and Molecular Engineering, Peking University, Beijing 100871, China;
[2] Nanotechnology Industrialization Base of China, Tianjin 300457, China

**We report herein a rational approach for fabricating metal suspending nanostructures by nanoimprint lithography (NIL) and isotropic reactive ion etching (RIE). The approach comprises three principal steps: (1) mold fabrication, (2) structure replication by NIL, and (3) suspending nanostructures creation by isotropic RIE. Using this approach, suspending nanostructures with Au, Au/Ti or Ti/Au bilayers, and Au/Ti/Au sandwiched structures are demonstrated. For Au nanostructures, straight suspending nanostructures can be obtained when the thickness of Au film is up to 50 nm for nano-bridge and 90 nm for nano-finger patterns. When the thickness of Au is below 50 nm for nano-bridge and 90 nm for nano-finger, the Au suspending nanostructures bend upward as a result of the mismatch of thermal expansion between the thin Au films and Si substrate. This leads to residual stresses in the thin Au films. For Au/Ti or Ti/Au bilayers nanostructures, the cantilevers bend toward Au film, since Au has a larger thermal expansion coefficient than that of Ti. While in the case of sandwich structures, straight suspending nanostructures are obtained, this may be due to the balance of residual stress between the thin films.**

suspending nanostructure, fabrication, nanoimprint lithography (NIL), isotropic reactive ion etching (RIE)

## 1 Introduction

Micro-electromechanical systems (MEMS) have wide applications in the development of cantilever sensors for detection in many fields[1]. A reduction of the dimensions of the mechanical sensor leads to a new generation of systems called nano-electromechanical systems (NEMS)[2,3], which represents an improvement on sensitivity, spatial resolution, integration, energy efficiency and time of response. So far, applications of nano-cantilever sensors are mainly focused on dynamic mode silica based nano-sensors (nano-resonator) used as mass sensors. The principle of nano-resonator is based on vibrating the cantilever and detecting the cantilever resonance frequency shift due to mass changes of the cantilever, e.g. due to adsorption of molecules. Such systems can benefit significantly from miniaturization, e.g. by simply reducing the dimensions of the cantilever to nanometre scale. Davis's research group[3−8] has described effort to develop a silicon based nano-resonator system directly integrated on a pre-processed CMOS chip. A mass sensitivity of around $10^{-19}$g is expected to obtain, which is high enough to detect changes in mass corresponding to a single biomolecule. Gupta et al.[9] have recently fabricated silicon based microresonators with thickness of 20—30 nm, and have successfully used the resonators to detect single virus particle.

Received September 26, 2007; accepted July 31, 2008; Published online January 12, 2009
doi: 10.1007/s11431-008-0290-7
†Corresponding authors (email: Xie_guoyong@163.com; ZFLiu@pku.edu.cn)
Supported by the National Natural Science Foundation of China (Grant No. 20573002) and the Major State Basic Research Development Program of China (973Pprogram) (Grant No. 2001CB6105)

Previous attempts at fabricating submicron scale suspending structures include electron beam lithography (EBL), Atomic Force Microscopy lithography, and directing writing laser lithography (DWL), combined with wet etching[3,6,8]. However, the throughput of the aforementioned lithography techniques is very low and these techniques are not very suitable for a mass fabrication of nano-cantilever sensors. What is more, the use of wet etching for the definition and release of suspending nanostructures is problematic[10—13]. First, KOH broadens the line width of the defined structures due to the anisotropic etch profile and second, the released structures might stick to the underlying substrate due to capillary forces, hydrogen bridging, electrostatic forces and van der Waals forces.

Nanoimprint lithography (NIL) has been proposed by Chou et al.[14—16] as an alternative approach for fabrication of nanostructures with critical dimensions in the sub-100 nm range at the wafer scale level, which is based on compression molding and pattern transfer process. In the imprint process, a mold with nanostructures on its surface is pressed into a thin resist cast on a substrate. The resist, a thermal plastic, is deformed readily by the mold when being heated above its glass transition temperature (due to a low viscosity). After the resist is cooled below its glass transition temperature, the mold is removed. In the following pattern transfer process, an anisotropic etching process, such as anisotropic reactive ion etching (RIE), is used to remove the residual resist in the compressed area, transferring the thickness contrast pattern created in the imprint into the entire resist. Compared with EBL, SPL and DWL, NIL offers a low cost method for mass producing nanostructures. Here, we report on the fabrication of suspending metal nanostructures using NIL and sequent isotropic RIE.

## 2 Fabrication procedures

The schematic diagram of the fabrication procedure is shown in Figure 1, which comprises of three principal steps: (1) mold fabrication by EBL; (2) structure replication by NIL; and (3) suspending nanostructures creation by isotropic RIE. Au and Ti are demonstrated as monolayer, bilayer and sandwiched cantilevers.

The first step in fabrication was to make imprint molds using EBL and RIE. Two kinds of patterns were designed, nano-finger and nano-bridge patterns. The nano-finger patterns had line width of 100, 200, 300 and 500 nm, respectively, and with length ranging from 2 μm to 12 μm. Each nano-bridge pattern has lines with width of 100, 200, 300 and 500 nm, with length ranging from 4 μm to 16 μm. 10 mm×10 mm Si wafers with 600-nm thick thermal $SiO_2$ are used. The wafers were spin coated with ~150 nm PMMA resists, exposed with EBL at 35 keV with a probe current of 20 pA. After resist development, 2-nm-thick Ti and 25-nm-thick Au were thermally evaporated and lifted off in warm acetone. Ultrasonic agitation was used in the lift-off procedure. The Ti+Au layer (Ti served as adhesion layer) was then used as an etch mask in reactive ion etching of $SiO_2$ in Ar/$CHF_3$ chemistry for 120 s (Ar 25 sccm, $CHF_3$ 25 sccm, 30 mTorr, 15 W). Immediately after the reactive ion etching, the metal mask was removed and the $SiO_2$ surface was treated by vapor deposition of tridecafluoro

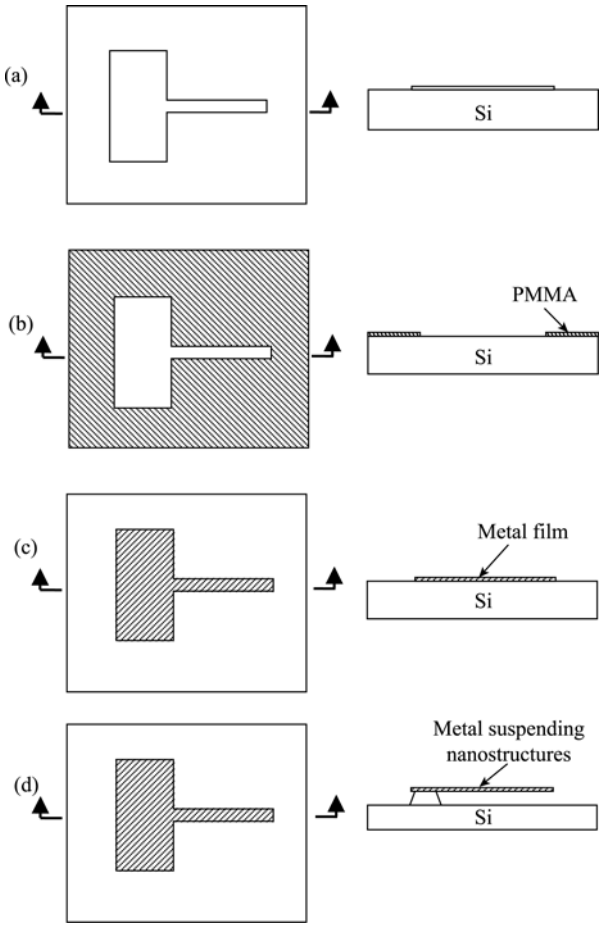


**Figure 1** Schematic diagram of the procedures for fabricating suspending metal nanostructures by nanoimprint lithography and isotropic reactive ion etch. Mold is first defined by EBL (a), then the patterns on the mold is imprinted in PMMA coated on Si substrate (b). Metal was thermally evaporated and lifted off in warm acetone, forming metal patterns on the Si substrate (c). Finally, suspending nanostructures are released by isotropic reactive ion etch (d).

(1, 1, 2, 2-) tetrahydrooctyl trichlososilane ($F_{13}$-TCS) to prevent sticking of resist to the stamp. SEM images of a nano-finger pattern with 300 nm line in width and a nano-bridge pattern with 8 μm in length are shown in Figure 2(a) and (b). The protrusion on the mold is approximately 120 nm high.

For the NIL experiments, Si wafers were spin coated with ~150 nm thick PMMA (MW 5000) and imprinted at 45 bar and 200℃ for 300 s. After printing, the wafers were exposed to oxygen plasma ($O_2$ 20 sccm, 30 mTorr, 15 W) for 40 s to remove residual PMMA in the patterned regions. Then metals, Au or Cr used as materials of suspending nanostructures, were thermally evaporated and then lifted off in warm acetone, forming metal patterns on the Si substrate. Finally, isotropic reactive ion etching was performed to etch Si substrate with $SF_6/O_2$ ($SF_6$ 30 sccm, $O_2$ 5 sccm, 80 mTorr and 100 W) for 60 s to release the suspending nanostructures. $SF_6/O_2$ chemistry performs almost isotropic etching for Si substrate, and shows high etching selectivity between Si and metal mask, which resulted in severe undercut during etching. The Si under the metal mask was etched gradually, and the metal cantilever was fully suspended at last.

An ultrahigh resolution electron beam lithography patterning tool (Raith 150) was used to fabricate $SiO_2$/Si molds for nanoimpint. Metal thermal evaporation was carried out using a BOC EDWARDS AUTO306 evaporator. Imprinting work was done on an Obducat Nanoimprinter with a 60-mm-diam substrate holder, and reactive ion etching was performed on an Oxford 80Plus RIE. The SEM images were taken with a LEO 1530 VP scanning electron microscope (LEO Elektronenmikroskopie GmbH, Oberkochen, Germany).

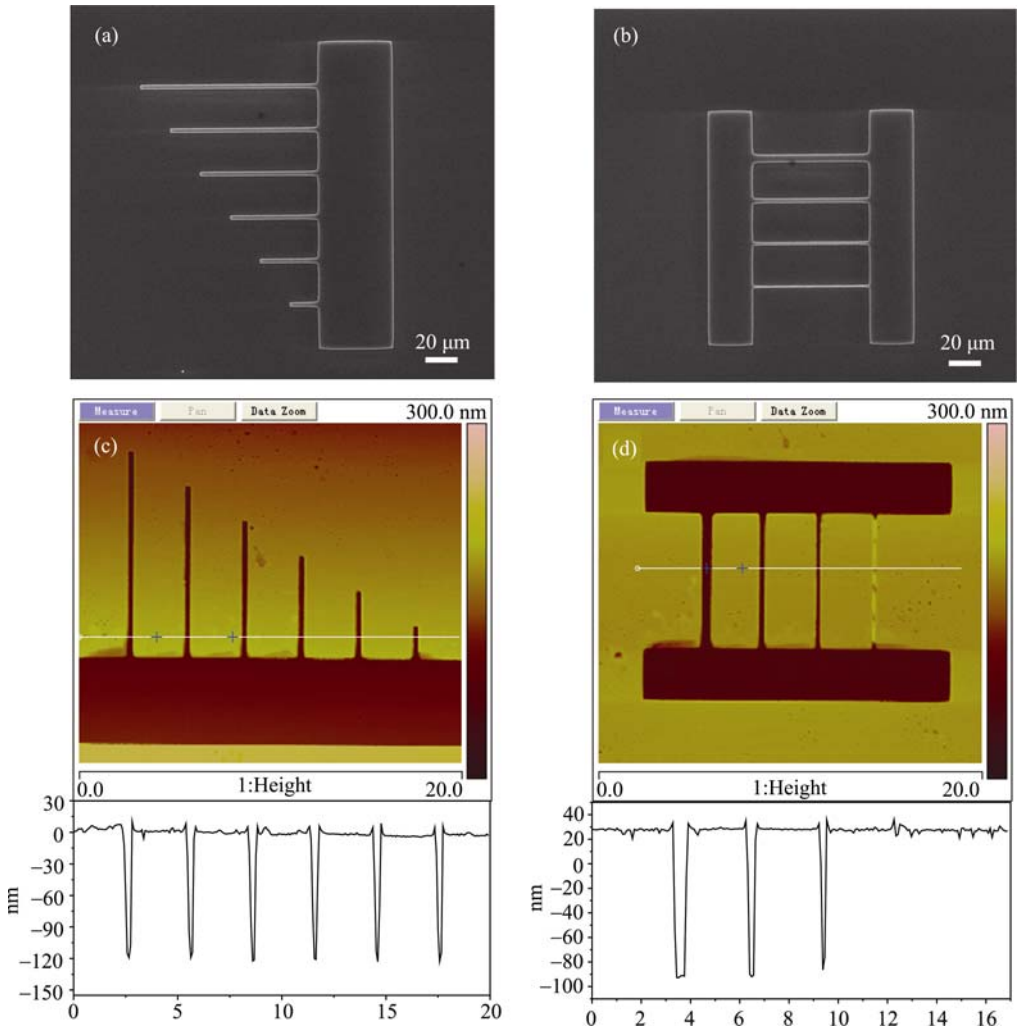


**Figure 2** SEM images of mold (a, b) and AFM images of corresponding nanoimprint results (c, d). (a, c) Nano-finger pattern with line width of 300 nm and length ranging from 2 μm to 12 μm; (b, d) nano-bridge pattern with lines width of 100, 200, 300 and 500 nm and length of 8 μm.

## 3 Results and discussion

### 3.1 Results of nanoimprint

The typical AFM (Nanoscope V, DI) images of the replicated nano-finger (with 300 nm line width) and nano-bridge (with 8 μm long) patterns are shown in Figure 2 (c) and (d). It can be seen that the replicated patterns show excellent surface uniformity over the area that is imprinted. The geometry of the patterned PMMA surface is in close agreement with that expected from that of the original mold (patterns in Figure 2 (a) and (b)). This indicates that NIL is competent for pattern definition in the fabrication of suspending nanostructures. It can also be found that the 100-nm-wide line in the nano-bridge pattern is not replicated (Figure 2(d)). Characterization of the post-imprinted mold shows that the 100-nm-wide lines are absent. This indicates that the 100-nm-wide lines have been destroyed during the imprinting process, which may be due to undercut RIE during mold fabrication.

### 3.2 Results of suspending nanostructures fabrication

3.2.1 Monolayer suspending metal nanostructures.

Figures 3 and 4 show the SEM images of monolayer metal suspending nanostructures. The thickness of Au films ranges from 17 to 90 nm, and a 2-nm thick Ti layer is used as adhesion layer for Au deposition. It can be seen from Figure 3 that the nanocantilevers with 17 nm thick Au (Figure 3(a)) coil upward. This may be mainly due to the mismatch of thermal expansion between the thin Au films and the Si substrate, which may lead to residual stresses in the thin Au films[17].

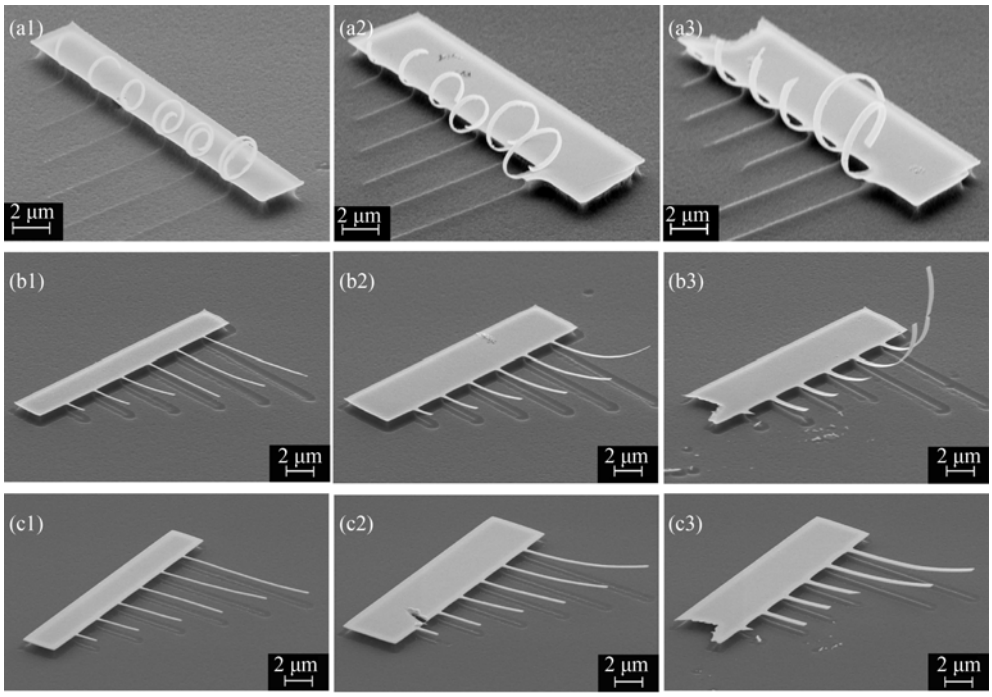


**Figure 3** SEM images of monolayer suspending nano-finger patterns with line width of 200, 300 and 500 nm from left to right, as a function of Au layer thickness. (a) 17-nm-thick Au, (b) 50-nm-thick Au, (c) 90-nm-thick Au. 2-nm-thick Ti is deposited between Au film and substrate Si as adhesion layer.

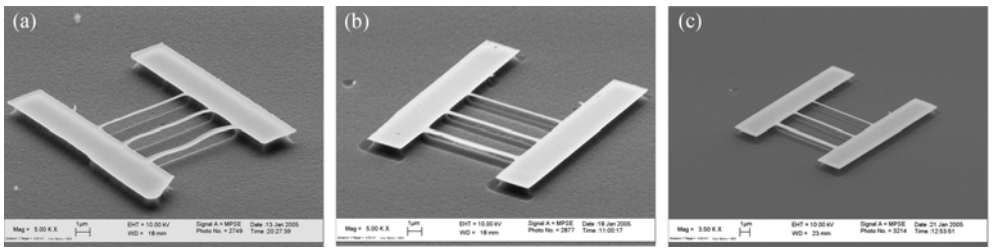


**Figure 4** SEM images of monolayer suspending nano-bridge patterns, with length of 8 μm, as a function of Au layer thickness. (a) 17-nm-thick Au, (b) 50-nm-thick Au, (c) 90-nm-thick Au. 2-nm-thick Ti is deposited between Au film and substrate Si as adhesion layer.

Residual stress in thin film, mainly resulting from mismatch of thermal expansions between different materials, is an important mechanical behavior in the areas of MEMS and NEMS. For a thin film with an effective young's mould $E_S$ and an effective thermal expansion coefficient $\alpha_1$, the residual stress $\sigma_{th}$ which arises from a temperature increase $\Delta T$ can be expressed as eq. (1)[17].

$$\sigma_{th} = E_S \cdot \varepsilon_{th} = E_S(\alpha_1 - \alpha_2)\Delta T, \quad (1)$$

where $\alpha_2$ denotes the thermal expansion coefficient of the substrate, and $\varepsilon_{th}$ denotes the corresponding elastic deformation. If $\alpha_1 > \alpha_2$, the thin film is under residual compression. Otherwise, the thin film is under residual tension in the case of $\alpha_1 < \alpha_2$. Effects of the residual tress in thin film are in two-fold: on the one hand, the micromachined or nanomachined structures may be damaged or deformed with release of residual tress[18]; on the other hand, the residual tress can be exploited to drive microactuators or nanoactuators[19, 20].

It is interesting to note that the curvatures radius of the cantilevers in Figure 5 increases with the increase of Au film thickness. When the thickness of the Au film reaches to 90 nm, slight bent effect can be found. Cantilevers shorter than 8 μm are nearly straight. It is reported that the curvature radius ρ of the deformed film can be expressed as[21]

$$\rho = \frac{2h}{3(\alpha_1 - \alpha_2)}\Delta T, \quad (2)$$

where $h$ denotes the film thickness. If the thermal expansion coefficient mismatch between the two thin films ($\alpha_1$–$\alpha_2$) is stable, curvature radius $\rho$ is directly proportional to the film thickness $h$. This may be a reasonable explanation for the above results. For suspending nano-bridge structures, as shown in Figure 4, straight beams are obtained when the thickness of Au film reaches up to 50 nm. Hence, straight nanocantilevers can be obtained by increasing film thickness. From Figures 3 and 4, it can also be found that stiction of suspending nanostructures to substrate is not observed, which indicates that isotropic RIE is suitable to releasing suspending nanostructures.

3.2.2 Bilayer suspending metal nanostructures. Based on the fact that mismatch of thermal expansion between different thin films may lead to deformation of nanocantilever, Au/Ti or Ti/Au bilayers, and Au/Ti/Au multi-sandwich-layer structures were used to fabricate nanocantilevers with anticipative shape. SEM images in Figure 5 are the fabrication results of bilayer nanocantilevers. All the bilayer nanocantilevers have a total thickness of 100 nm, 50-nm-thick Au and 50-nm-thick Ti. Figure 5 shows that the nanocantilevers bend downward when the Ti film is deposited on the top of Au film, whereas the bend orientation is inverse when the Au film is deposited on the top of Ti film. In other words, the nanocantilevers bend toward Au side. It is known that bulk Au has a larger thermal expansion coefficient ($14\times10^{-6}$ ℃$^{-1}$) than that of bulk Ti ($8.2\times10^{-6}$ ℃$^{-1}$). According to eq. (1), the Au film is under residual tension, and the Ti film is under residual compression, which is the reason for nanocantilever's curving toward Au side.

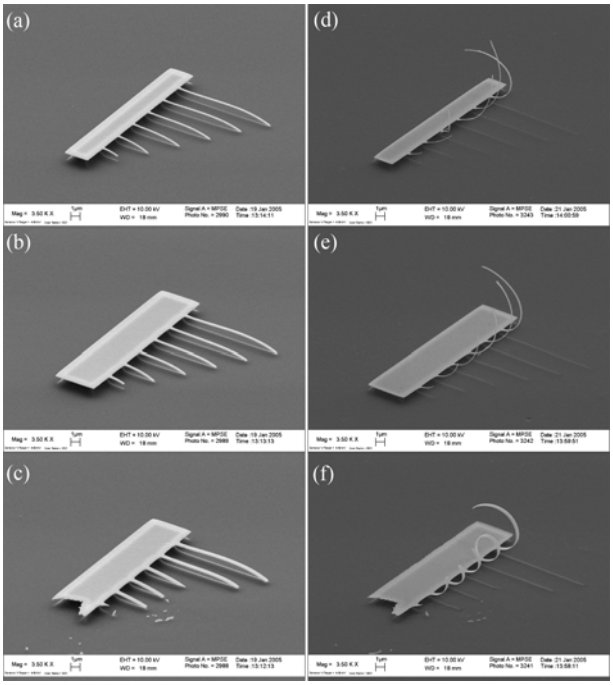


**Figure 5** SEM images of bilayer suspending nano-finger patterns. (a), (b), (c) 50-nm-thick Ti deposited on 50-nm-thick Au (50nmAu+50nmTi), with line width of 200, 300 and 500 nm, respectively; (d), (e), (f) 50-nm-thick Au deposited on 50-nm-thick Ti (50nmTi+50nmAu), with line width of 200, 300 and 500 nm, respectively.

3.2.3 Multi-sandwich-layer suspending metal nanostructures. Figure 6 shows the results of multi-sandwich-layer nanocantilevers. Two kinds of 100-nm-thick sandwiched structures are designed, (1) Ti layer is sandwiched with Au layers (25 nmAu+50 nmTi+25 nmAu) (Figure 6(a), (b), (c)); (2) Au layers and Ti layers are sandwiched with each other (20nmAu+20nmTi+20nmAu +20nmTi+20nm Au) (Figure 6(e)). It can be seen that nearly straight shape is obtained for these sandwiched structures. This indicates that, in the sandwiched structures, the residual tress of side layers may be balanced in

the middle layer. Cantilevers with line width of 500 nm are completely straight, as shown in Figure 6(c) and (d). However, slightly downward curve at tips can be found for the cantilevers with line width of 200 and 300 nm, which may be due to boundary or tip effect existing in nano- scale structures. Anyway, unpredictable factors in the experiment may also affect the results. From the aforementioned results, straight nanocantilevers may be fabricated by changing metal film deposition sequence or film thickness, considering the residual stress in thin film.

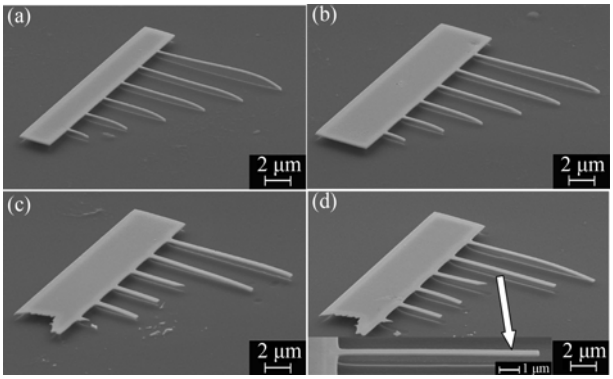


**Figure 6** SEM images of multi-sandwich-layer suspending nano-finger patterns. Two kinds of 100-nm-thick sandwiched structures are designed, (a), (b), (c) Ti layer is sandwiched with Au layers (25nmAu+50nmTi+25nmAu) with line width of 200, 300 and 500 nm, respectively; (d) Au layers and Ti layers are sandwiched with each other (20nmAu+20nmTi+20nmAu+20nmTi+20nmAu) with line width of 500 nm.

## 4 Summary

In conclusion, we have described a simple and low cost method for the fabrication of suspending metal nanostructures. Nanoimprint lithography is used as a mask definition technique with the advantage of low cost and high throughput. Isotropic reactive ion etch is effectively used to release suspending nanostructures, which avoids the problems met in wet etching. Nanocantilever shape is controlled by designing the metal deposition sequence and film thickness, considering mismatch of thermal expansion between different thin films.

The suspending metal nanostructures may be used both as nanoresonators and nanoactuators with high sensitivity. Furthermore, nanoimprint lithography and reactive ion etching are metal-oxide-semiconductor (CMOS) compatible, which makes it possible to fabricate suspending metal nanostructures with integrated microelectronics.


1 Brand O, Baltes H. Sensors, vol 4. New York: Wiley, 1998
2 Craighead H G. Nanoelectromechanical systems. Science, 2000, 290: 1532－1535
3 Forsen E, Nilsson S G, Carlberg P, et al. Fabrication of cantilever based mass sensors integrated with CMOS using direct write laser lithography on resist. Nanotechnology, 2004, 15: S628－633
4 Boisen A, Birkelund K, Hansen O, et al. Fabrication of submicron suspended structures by laser and atomic force microscopy lithography on aluminum combined with reactive ion etching. J Vac Sci Technol B, 1998, 16 (6): 2977－2981
5 Abadal G, Boisen A, Davis Z J, et al. Combined laser and atomic force microscope lithography on aluminum: Mask fabrication for nanoelectromechanical systems. Appl Phys Lett, 1999, 74 (21): 3206－3208
6 Davis Z J, Abadal G, Kuhn O, et al. Fabrication and characterization of nanoresonating devices for mass detection. J Vac Sci Technol B, 2000, 18 (2): 612－616
7 Abadal G., Davis Z J, Helbo B, et al. Electromechanical model of a resonating nano-cantilever-based sensor for high-resolution and high-sensitivity mass detection. Nanotechnology, 2001, 12: 100－104
8 Ghatnekar-Nilsson S, Forsen E, Abadal G, et al. Resonators with integrated CMOS circuitry for mass sensing applications, fabricated by electron beam lithography. Nanotechnology, 2005, 16: 98－102
9 Gupta A, Akin D, Bashir R. Single virus particle mass detection using microresonators with nanoscale thickness. Appl phys Lett, 2004, 84 (11): 1976－1978
10 Mastrangelo C H, Hsu C H. Mechanical stability and adhesion of microstructures under capillary forces. J Microelectromech Syst, 1993, 2: 33－55
11 Tas N, Sonnenberg T, Jansen H, et al. Stiction in surface micromachining. J Micromech Microeng, 1996, 6: 385－397
12 Bartek M, Wolffenbuttel R F. Dry release of metal structures in oxygen plasma: process characterization and optimization. J Micromech Microeng, 1998, 8: 91－94
13 Forsen E, Davis Z J, Dong M, et al. Dry release of suspended nanostructures. Microelect Eng, 2004, 73-74: 487－490
14 Chou S Y, Krauss P R, Renstrom P J. Imprint of sub-25 nm vias and trenches in polymer. Appl Phys Lett, 1995, 67 (21): 3114－3116
15 Chou S Y, Krauss P R, Renstrom P J. Imprint lithography with 25-nanometer resolution. Science, 1996, 272 (5258): 85－87
16 Chou S Y, Keimel C, Gu J. Ultrafast and direct imprint of nanostructures in silicon. Nature, 2002, 417 (6891): 835－837
17 Madau M. Fundamentals of Microfabrication. Boca Raton: CRC Press, 1997
18 Suh J W, Glander S F, Darling R B, et al. Organic thermal and electrostatic ciliary microactuator array for object manipulation. Sensors and Actuators A, 1997, 58: 51－60
19 Kohl M, Skrobanek K D, Miyazaki S. Development of stress-optimized shape memory microvalves. Sensors and Actuators A, 1999, 72: 243－250
20 Fu Y, Du H, Huang W, et al. TiNi-based thin films in MEMS applications: a review. Sensors and Actuators A, 2004, 112: 395－408
21 Hsu T R. MENS & Microsystems: Design and Manufacture. Beijing: McGraw-Hill Education Co. and China Machine Press, 2004. 127